

Supporting Information

“Colored” inorganic dopants for inducing liquid crystal chiral nematic and blue phases: monitoring of dopant-host interaction by Raman spectroscopy

Jun Yoshida,^{a*} Shuhei Tamura,^a Go Watanabe,^{b*} Yasutoshi Kasahara,^a and Hidetaka Yuge^a

^aKitasato University, Department of Chemistry, School of Science, Kitasato 1-15-1, Sagamihara, Japan.

^bKitasato University, Department of Physics, School of Science, Kitasato 1-15-1, Sagamihara, Japan.

Contents

Physical measurements and materials	2
Synthesis	3
¹ H NMR spectrum	7
APCI-MASS spectrum.....	8
Optical resolution by chiral HPLC	9
DFT calculations.....	11
HTP measurements	13
CD spectra.....	15
Transmission spectra.....	17
IR spectra	19
Raman spectra.....	21
Polarized optical microscope images.....	27

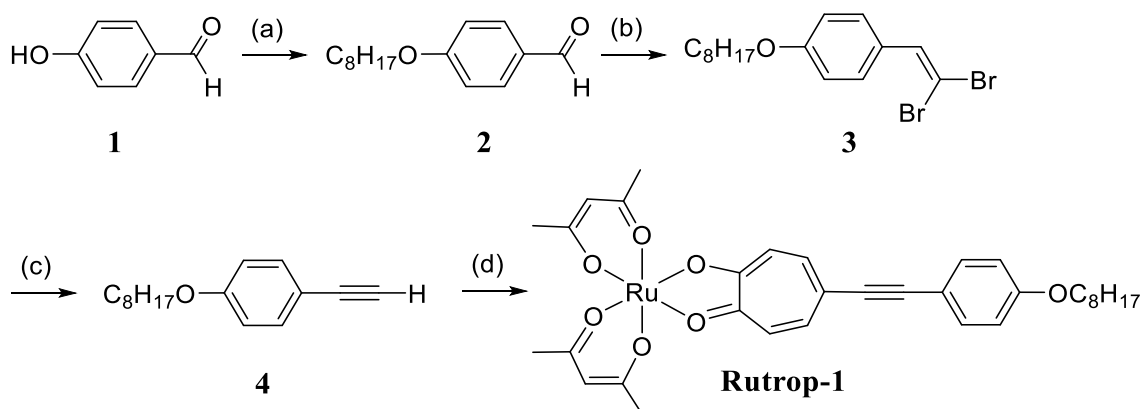
Physical measurements and materials

Physical measurements: ^1H NMR spectra were recorded at 600 MHz with a Bruker AVANCE-II-600. All spectra are referenced to tetramethylsilane. APCI mass spectrometry was performed with a Exactive Plus (Thermo Fisher Scientific); the mass range was 20–2000 with a nominal resolution (at m/z 200) of 140,000. Elemental analyses were carried out with a Perkin Elmer 2400II. UV-Vis and circular dichroism (CD) spectra were recorded with JASCO V-570 and J-720 spectrometers, respectively. The CD spectra of liquid crystal materials doped with enantiomeric Ru(III) complexes were measured using a homogeneous alignment cell of 10 or 25 μm thickness (RP type, EHC, Japan). Micro-Raman spectroscopy was performed with a JASCO NRS-7200 using green excitation (532 nm). Before the measurements, the Raman shift was calibrated with a silicon substrate. FT-IR spectroscopy was performed with a JASCO FT/IR-4200 with an ATR unit (diamond, MicromATR Vision, Czitek). Polarized optical microscope observation was performed with a CX-31 (Olympus) with transmitted and reflected light using a hot stage (Imoto Machinery).

Materials: tetrahydrofuran and dichloromethane were distilled over Na/benzophenone and CaH_2 , respectively, while other solvents employed were reagent grade. 1-bromooctane, CBr_4 , PPh_3 , $n\text{-BuLi}$, and N,N -diisopropylethylamine (DIPEA) were purchased from Kanto Chemical (Tokyo, Japan) or TCI (Tokyo, Japan) and used without further purification.

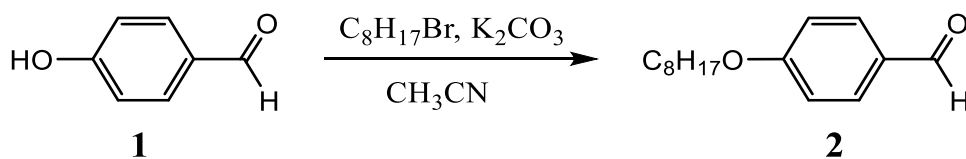
Synthesis

Ruthenium complex **Rutrop-1** was newly synthesized according to the procedure shown in Scheme S1. Alkyne **4** and $[\text{Ru}(\text{acac})_2(\text{Brtrop})]$ ($\text{BrtropH} = 5\text{-bromotropolone}$) were prepared following the previously reported procedure.^{1,2} The details of each synthetic condition are shown below.



Scheme S1 Reagents and conditions for the synthesis of **Rutrop-1**. (a) 1-bromooctane, K_2CO_3 , acetonitrile, (b) CBr_4 , PPh_3 , DCM (c) $n\text{-BuLi}$, THF, (d) $[\text{Ru}(\text{acac})_2(\text{Brtrop})]$, CuI (cat.), $[\text{PdCl}_2(\text{PPh}_3)_2]$ (cat.), THF, DIPEA.

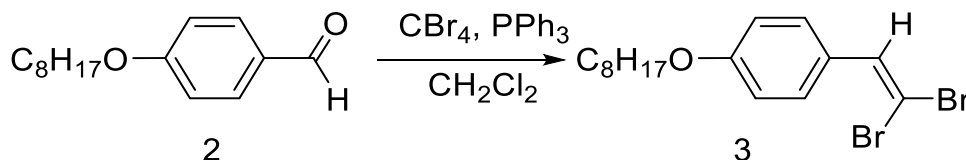
4-(*n*-octyloxy)benzaldehyde (**2**)



To an acetonitrile solution (200 ml), **1** (15.9 g, 117 mmol) and K_2CO_3 (19.3 g, 140 mmol) were added and the mixture was heated to reflux in nitrogen atmosphere. 1-bromooctane (20 ml, 115 mmol) were then added over 30 minutes, and the mixture was refluxed for additional 2 hours. After cooled to RT, the mixture was extracted by hexane three times and washed by NaOH solution (10 wt%). The organic layer was dried over Na_2SO_4 and then concentrated by rotary evaporator. **2** was obtained as yellow oil (25.3 g, 108 mmol, 92% yield).

1H NMR (600MHz, $CDCl_3$): δ = 0.89 (t, J = 7.0 Hz, 3H), 1.29 -1.38 (m, 8H), 1.47 (quin, J = 7.6 Hz, 2H), 1.80 (quin, J = 5.4 Hz, 2H), 4.02 (t, J = 6.6 Hz, 2H), 6.98 (d, J = 9.0 Hz, 2H), 7.81 (d, J = 9.0 Hz, 2H), 9.86 (s, 1H).

1-(2,2-dibromoethenyl)-4-(*n*-octyloxy)benzene (**3**)

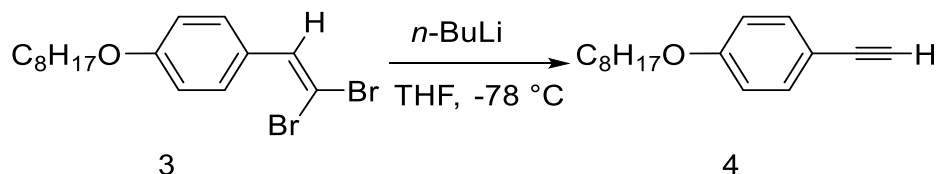


CBr_4 (37.3 g, 112 mmol) and PPh_3 (57.8 g, 220 mmol) were added to dichloromethane (180 ml) and stirred at 0 °C under nitrogen atmosphere for 30 minutes. To this solution, DCM solution (50 ml) containing **2** (13.0 g, 55.5 mmol) was slowly added and stirred at RT overnight. After the solution was filtered with Celite, the solvent was removed by rotary evaporator. The residue was subjected to SiO_2 column chromatography with hexane/DCM = 4/1 as an eluent. **3** was obtained as yellow oil (19.96 g, 51.2 mmol, 92% yield).

1H NMR (600MHz, $CDCl_3$): δ = 0.89 (t, J = 6.4 Hz, 3H), 1.27 - 1.36 (m, 8H), 1.41 - 1.48 (m, 2H), 1.78 (quin, J = 7.1 Hz, 2H), 3.96 (t, J = 6.6 Hz, 2H), 6.87 (d, J = 9.2 Hz, 2H), 7.40 (s, 1H), 7.50 (d, J

= 8.8 Hz, 2H).

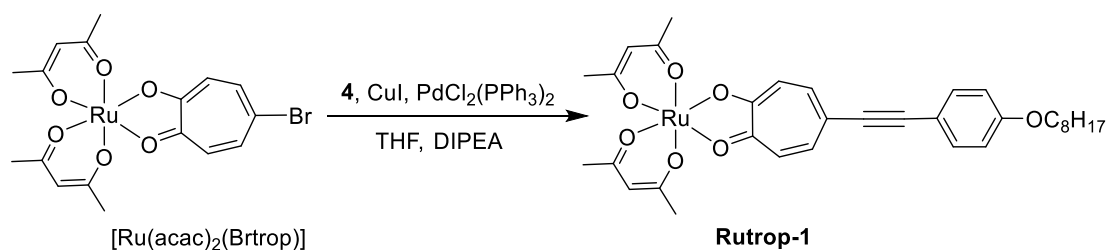
4-(*n*-octyloxy)phenylacetylene



A THF (250 ml) solution containing **3** (19.96 g, 51.2 mmol) was cooled to -78 °C. To this solution, *n*-BuLi (hexane solution, 40 ml, 64 mmol) was slowly added over 30 minutes. The mixture was stirred at -78 °C for additional 3 hours. At RT, saturated ammonium chloride solution (100 ml) was added to this solution. The mixture was extracted by ethyl acetate three times. The organic layer was dried over Na₂SO₄ and then concentrated by rotary evaporator. The residue was subjected to SiO₂ column chromatography with hexane/DCM = 4/1 as an eluent. **4** was obtained as yellow oil (10.53 g, 45.7 mmol, 89% yield).

¹H NMR (600MHz, CDCl₃): δ = 0.89 (t, *J* = 6.4 Hz, 3H), 1.25 - 1.36 (m, 8H), 1.42 - 1.47 (m, 2H), 1.75 (quin, *J* = 7.1 Hz, 2H), 2.98 (s, 1H), 3.95 (t, *J* = 6.6 Hz, 2H), 6.83 (d, *J* = 9.2 Hz, 2H), 7.41 (d, *J* = 8.8 Hz, 2H).

Rutrop-1



To a THF solution (140 ml), [Ru(acac)₂(Brtrop)] (300 mg, 0.601 mmol), DIPEA (1.00 ml, 5.73 mmol), CuI (29.4 mg, 0.154 mmol), [PdCl₂(PPh₃)₂] (43.8 mg, 0.0624 mmol) were successively added under nitrogen atmosphere. After the mixture was heated to 60 °C, a THF solution (5 ml) containing **4** (415 mg, 1.80 mmol) was slowly added. The mixture was further heated at 60 °C for additional 4 hours.

After the solvent was removed by rotary evaporator, the residue was subjected to SiO₂ column chromatography with DCM/CH₃CN = 20/1. **Rutrop-1** was obtained as brown solids (104 mg, 0.164 mmol, 27% yield).

¹H-NMR (600MHz, CDCl₃): δ = -37.13 (s, 2H), -13.70 (s, 6H), -8.04 (s, 6H), -6.44 (s, 2H), 0.90 (t, *J* = 6.9 Hz, 3H), 1.27-1.38 (m, 8H), 1.47 (quint, *J* = 7.7 Hz, 2H), 1.78 (quint, *J* = 7.2 Hz, 2H), 4.27 (t, *J* = 6.6 Hz, 2H), 5.28 (d, *J* = 8.4 Hz, 2H), 7.52 (d, *J* = 9.0 Hz, 2H), 11.68 (s, 2H).

Elemental analysis: Anal. Calc. for C₃₃H₃₉O₇Ru: C, 61.10; H, 6.06; Found: C, 61.32; H, 6.45.

HRMS (APCI⁺): calculated for C₃₃H₃₉O₇Ru ([M+H]⁺) *m/z* = 650.1821, found 650.1826.

¹H NMR spectrum

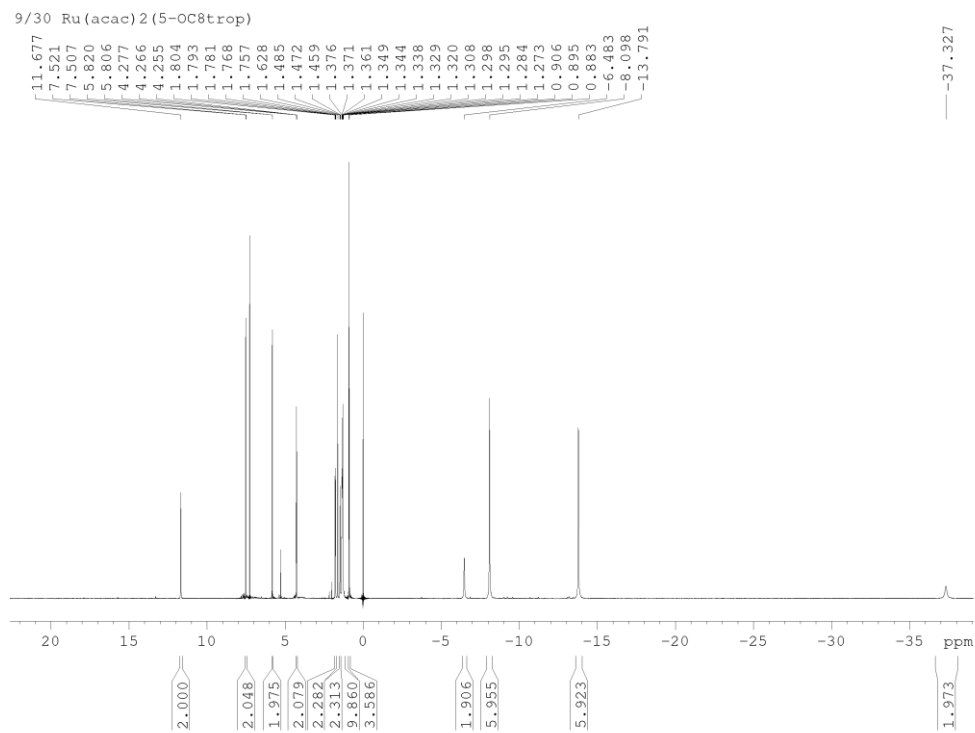


Figure S1 ¹H NMR spectrum of **Rutrop-1** measured in CDCl₃.

APCI-MASS spectrum

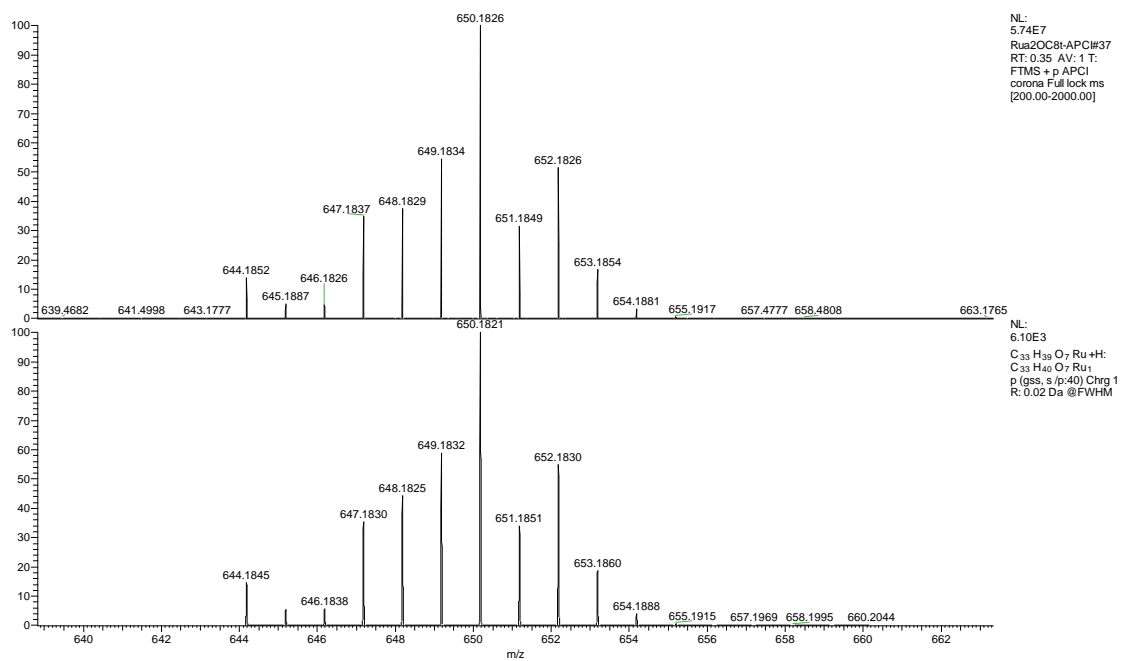


Figure S2 Experimental (top) and theoretical (bottom) isotopic patterns for [Rutrop-1 + H]⁺ (C₁₅H₂₁IO₆Ru).

Optical resolution by chiral HPLC

The optical resolution of **Rutrop-1** was performed by using recycling preparative HPLC (LC-9204, Japan Analytical Industry Co., Ltd.) with a semi-preparative chiral column (Chiralpak IA, Daicel Chemical Industries Co., Ltd.). As a mobile phase, *n*-hexane/chloroform (2/1, v/v) was used. Two well-separated major peaks were observed to the baseline separation in the 2nd Cycle (Figure S3). CD spectra of the less and more retained fractions are shown in Figure S4. From the comparison with Δ -[Ru(acac)₃] that shows the positive and negative Cotton effects at ca. 415 and 350 nm,^{3,4} less and more retained fractions were assigned to Λ and Δ isomers, respectively.

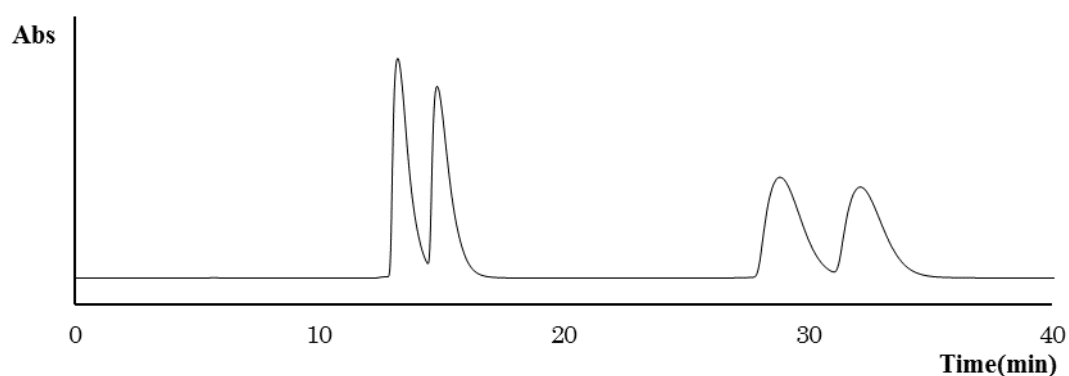


Figure S3 HPLC chromatogram of **Rutrop-1**. Chromatographic condition: CHIRALPAK 1A; *n*-hexane/chloroform = 2/1 (v/v); flow rate: 6 ml min⁻¹; detection 360 nm.

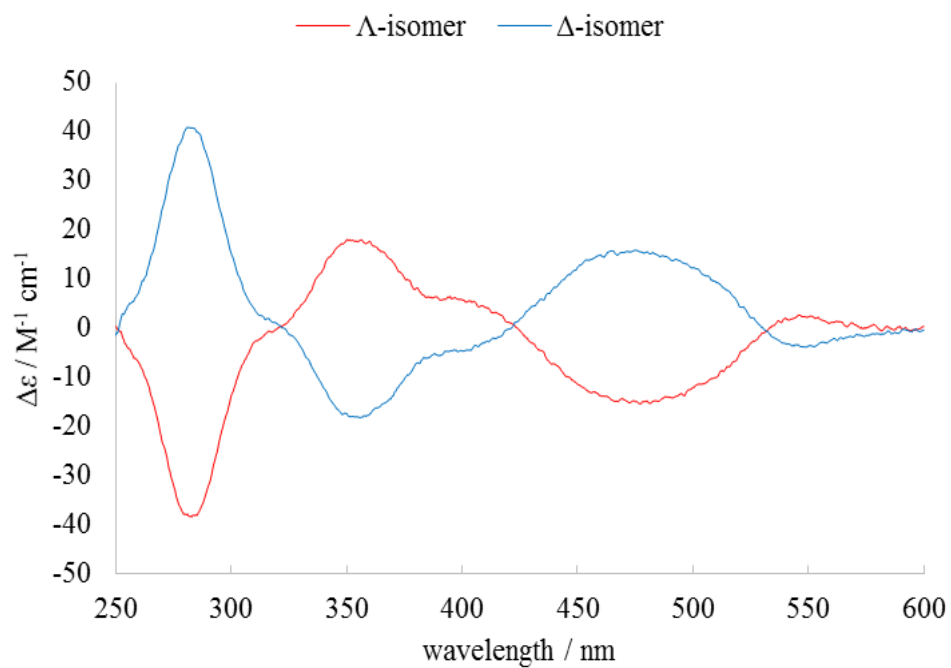


Figure S4 CD spectra of enantiomeric **Rutrop-1** measured in CHCl₃.

DFT calculations

Restricted and unrestricted DFT calculations of **5CB**, **Rutrop-1** and **Ruacac-1** were carried out to optimize structures and to calculate IR and Raman spectra. The calculation was performed using Gaussian 09 program⁶ using the density functional theory with B3LYP functional for the case of 5CB. The DFT calculation of **Rutrop-1** and **Ruacac-1** was performed at different functionals and basis sets (Conditions 01-06) as summarized in Table S1. Each optimized structure was confirmed to be a minimum by frequency calculation. In the Condition 06, solvent effect was included with the Polarizable Continuum Model (PCM)^{7,8} using dichloromethane as a solvent. Calculated IR and Raman spectra are shown in the following section with experimental spectra.

Table S1 Summary of DFT calculation conditions.

Condition	Functional	Basis sets	Comments
01	UCAM-B3LYP	6-31G(d) for C, H, O; LanL2DZ for Ru	
02	UB3PW91	6-31G(d) for C, H, O; LanL2DZ for Ru	
03	UWB97XD	6-31G(d) for C, H, O; LanL2DZ for Ru	
04	UMPW1PW91	6-31G(d) for C, H, O; LanL2DZ for Ru	
05	UMPW1PW91	6-311G(d) for C, H, O; LanL2DZ for Ru	
06	UMPW1PW91	6-311G(d) for C, H, O; LanL2DZ for Ru	Solvent effect (acetonitrile) was included.

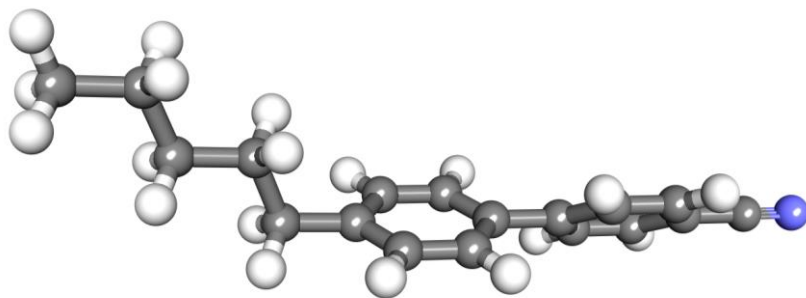


Figure S5 Optimized structure of **5CB** calculated with B3LYP functional and 6-31G(d) basis set.

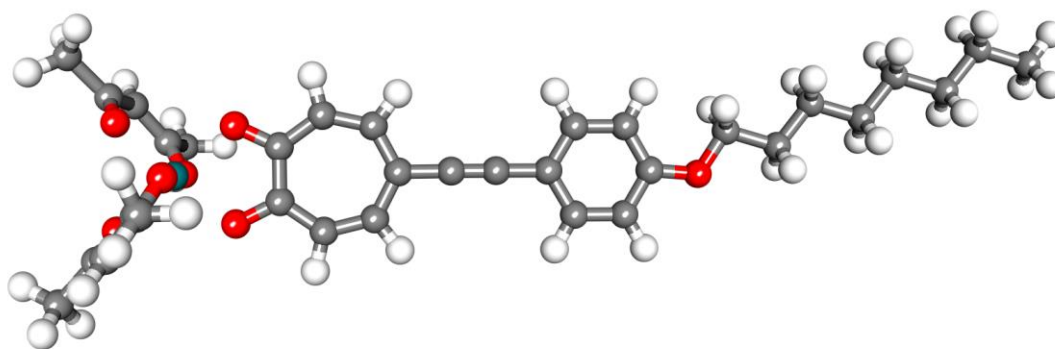


Figure S6 Optimized structure of **Rutrop-1** calculated with UMPW1PW91 functional and 6-311G(d) basis sets for C, H, O and LanL2DZ for Ru.

HTP measurements

Helical twisting powers of **Rutrop-1** were measured by the Cano method using a wedge cell (EHC, Japan).⁵ The schematic representation of a wedge cell is shown in Figure S7, where $\tan\theta$ equals to $p/2d$ or Y/X . After the liquid crystal samples were injected into the wedge cell, the cell was left for a few hours or overnight at RT to obtain uniform orientation. The measurements were done at 30 ± 0.1 °C by a self-made hot stage with a temperature control unit (E5CN, OMRON Inc.).

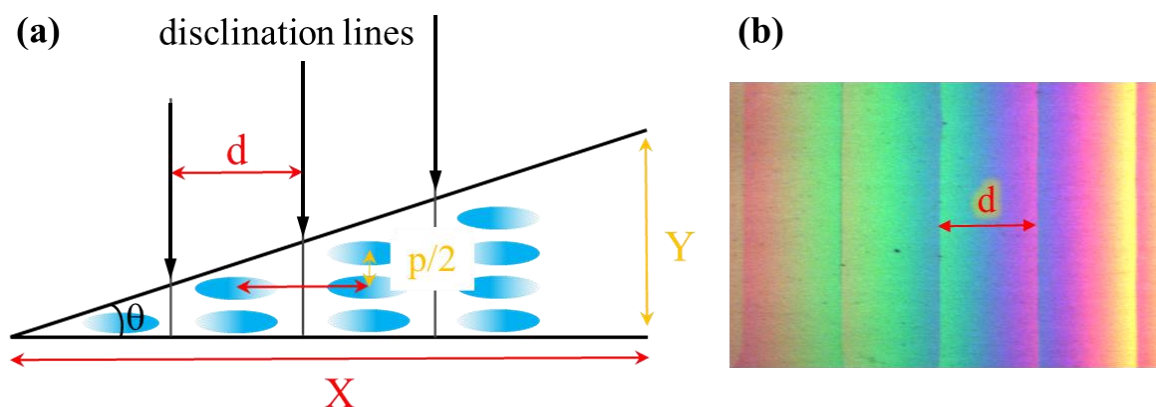


Figure S7 (a) Schematic representation of HTP measurement using a wedge cell. (b) Actual polarized microscope image of a wedge cell containing a chiral nematic liquid crystal.

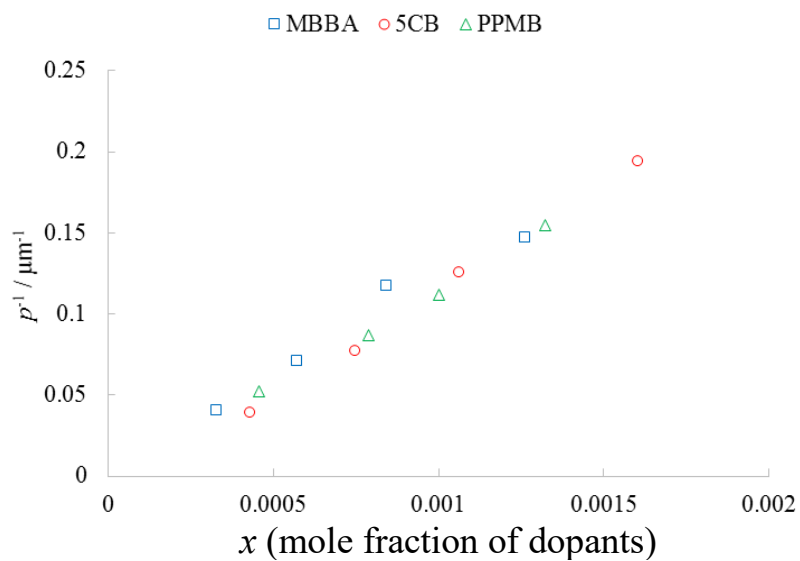


Figure S8 Plots of the inverse of helical pitch (p^{-1}) versus the mole fraction (x) of Δ -Rutrop-1 in MBBA, 5CB, and PPMB.

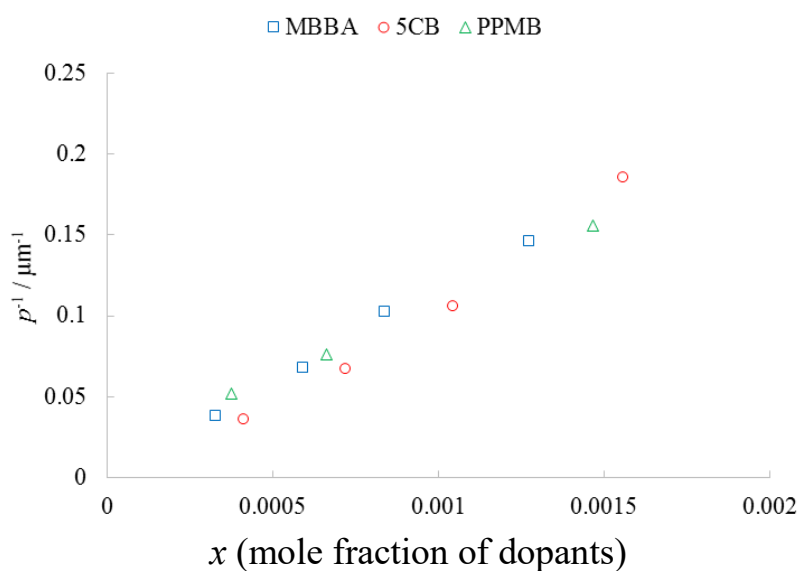


Figure S9 Plots of the inverse of helical pitch (p^{-1}) versus the mole fraction (x) of Λ -Rutrop-1 in MBBA, 5CB, and PPMB.

CD spectra

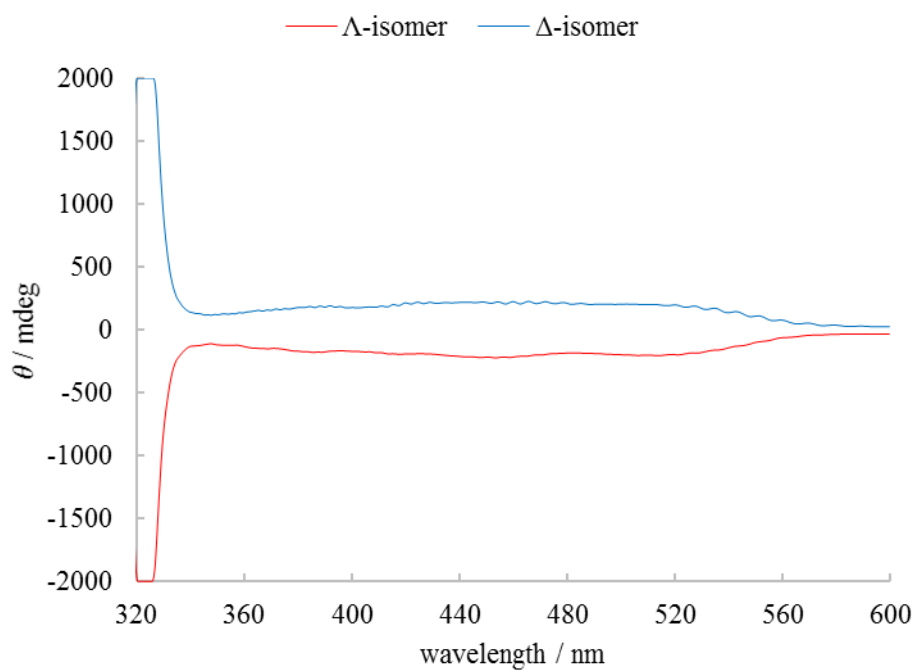


Figure S10 CD spectra of 5CB doped with Λ - and Δ -Rutrop-1 (ca. 0.04 mol%).

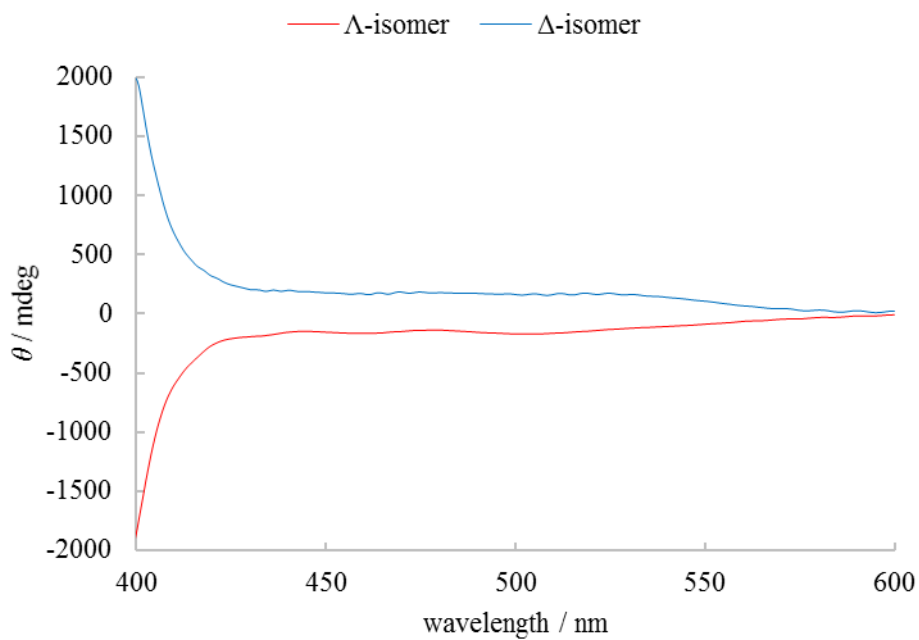


Figure S11 CD spectra of MBBA doped with Λ - and Δ -Rutrop-1 (ca. 0.04 mol%).

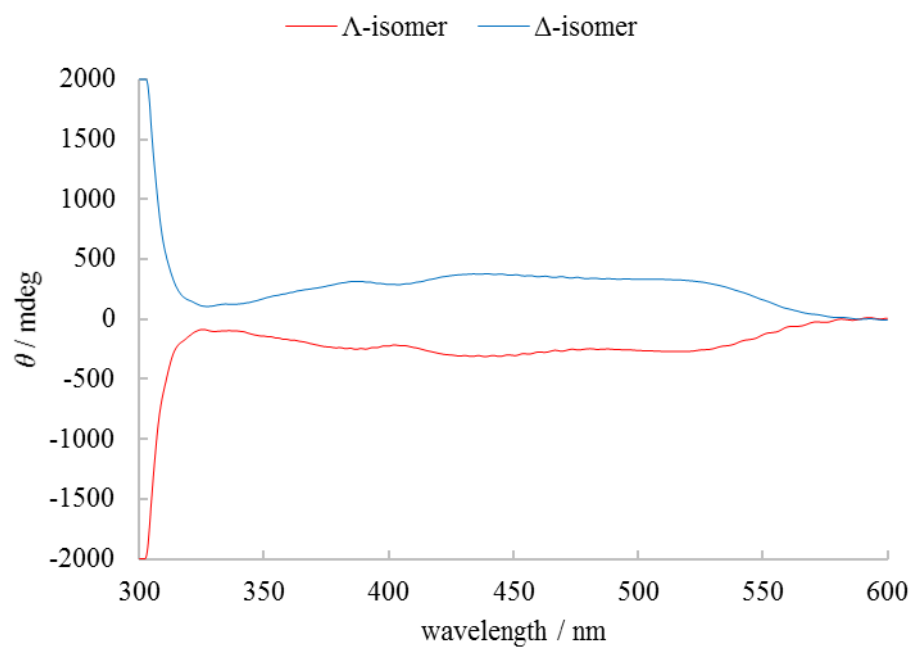


Figure S12 CD spectra of PPMB doped with Λ - and Δ -**Rutrop-1** (ca. 0.04 mol%).

Transmission spectra

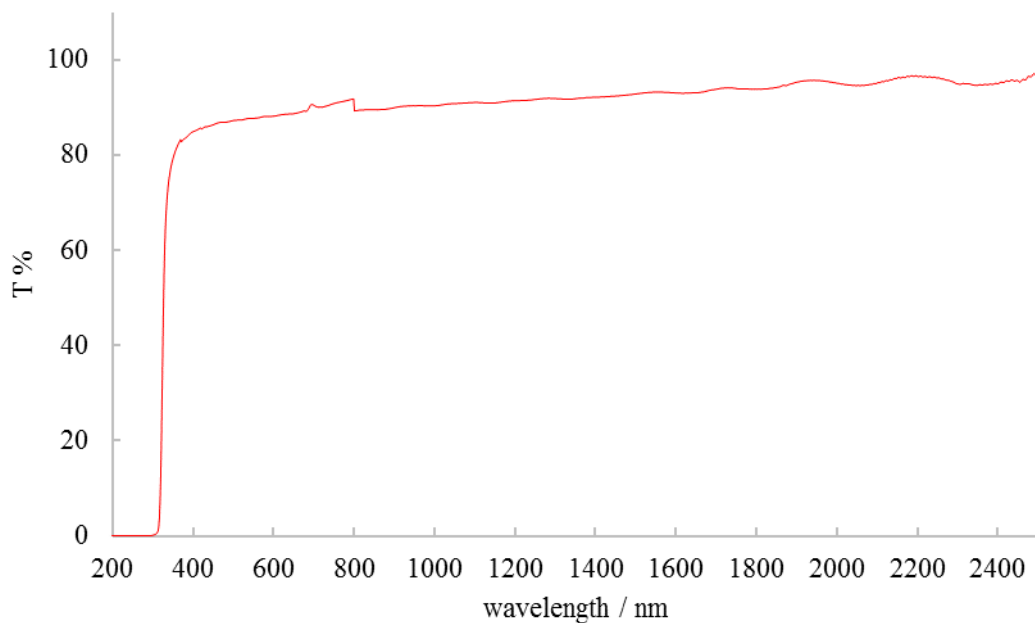


Figure S13 Transmission spectrum of 5CB in a homogeneous cell (10 μm).

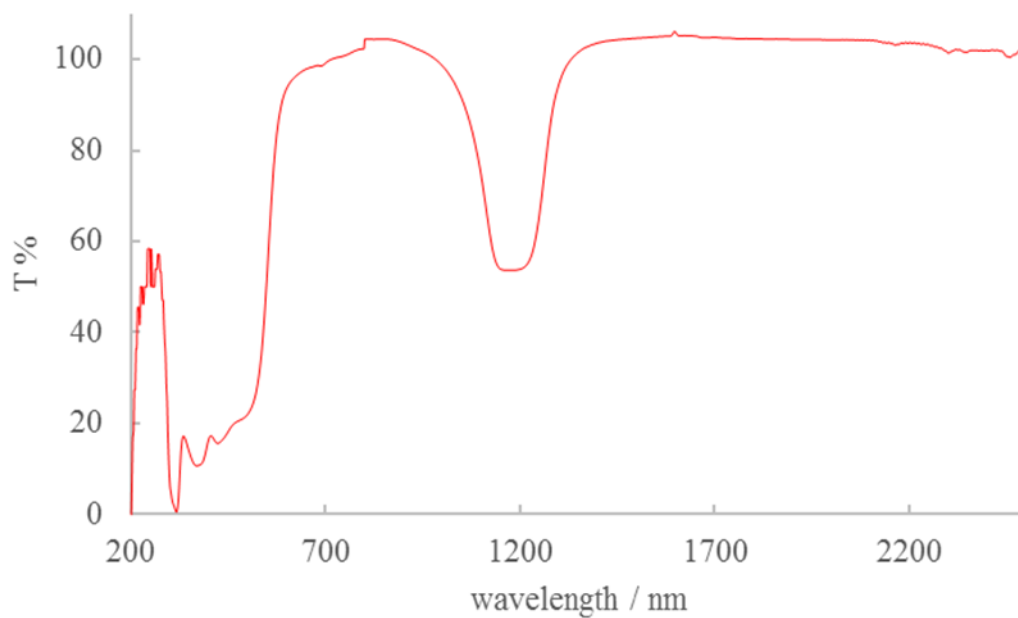


Figure S14 Transmission spectrum of the binary mixture of Δ -Rutrop-1 (1.0 mol%) and 5CB in a homogeneous cell (10 μm).

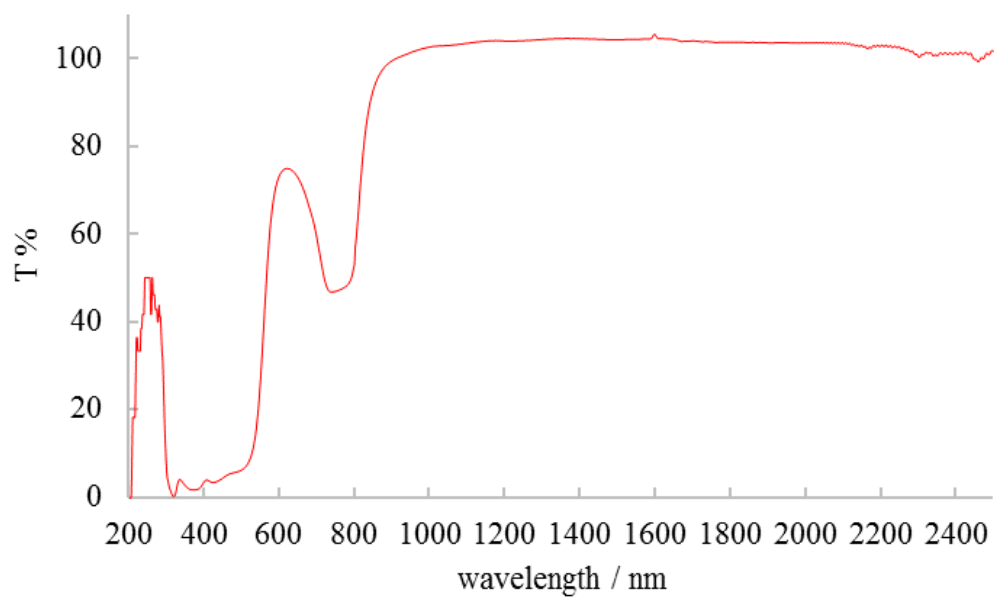


Figure S15 Transmission spectrum of the binary mixture of Δ -Rutrop-1 (1.4 mol%) and 5CB in a homogeneous cell (10 μm).

IR spectra

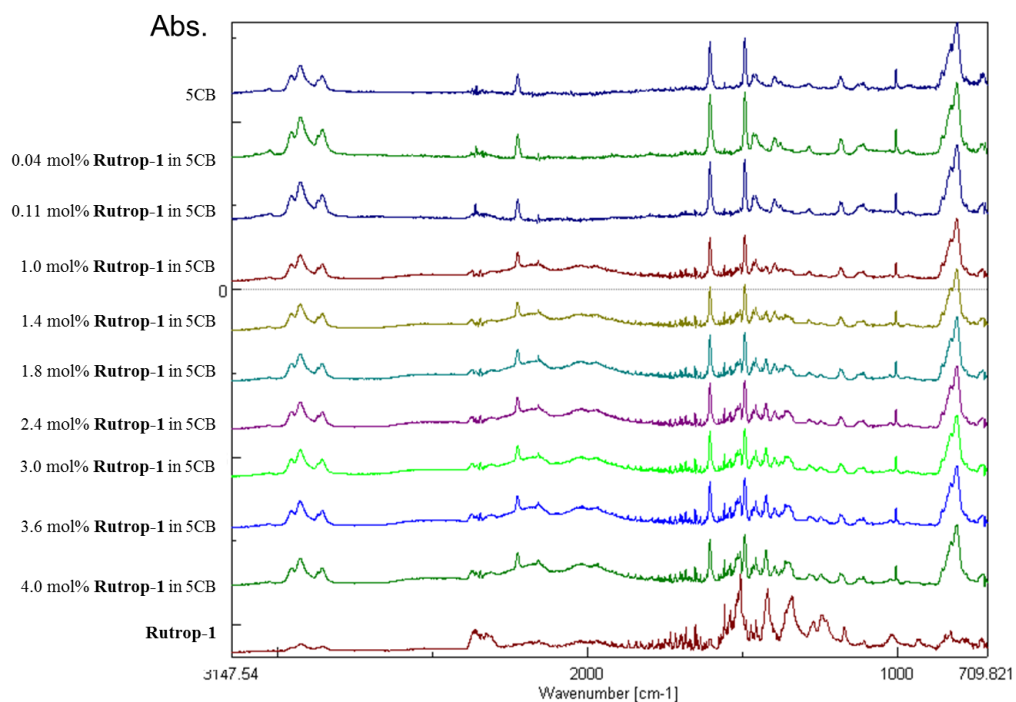


Figure S16 IR spectra of the binary mixtures of 5CB and Δ -Rutrop-1. Measurements were done at RT with an ATR unit.

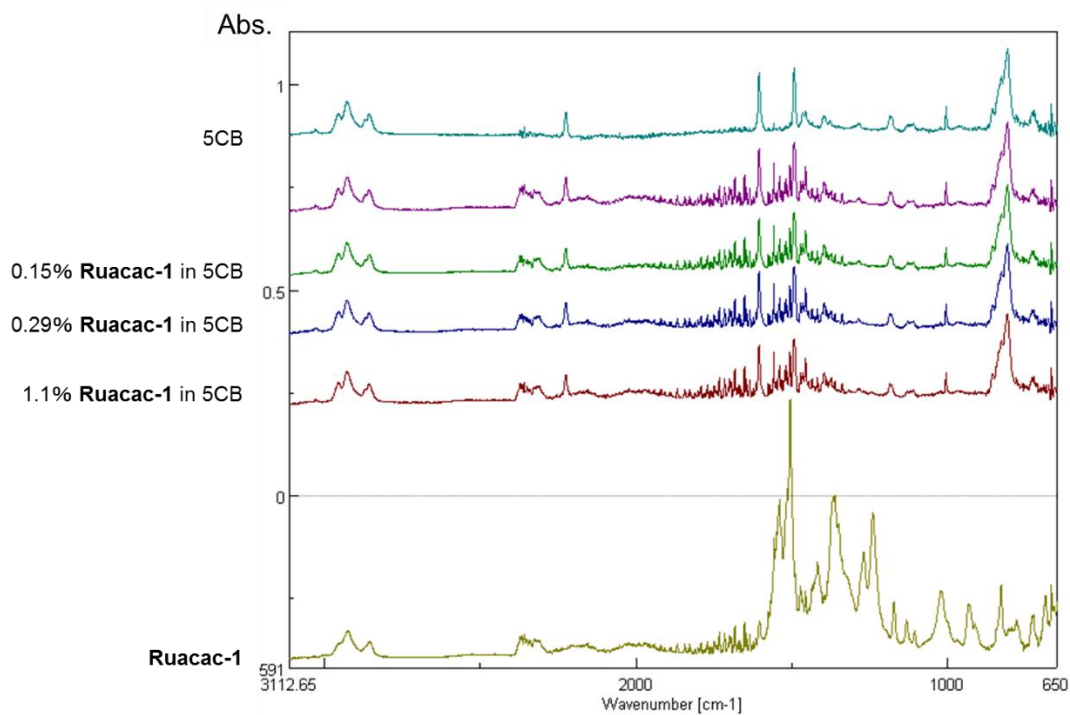


Figure S17 IR spectra of the binary mixtures of 5CB and Δ -Ruacac-1. Measurements were done at RT with an ATR unit.

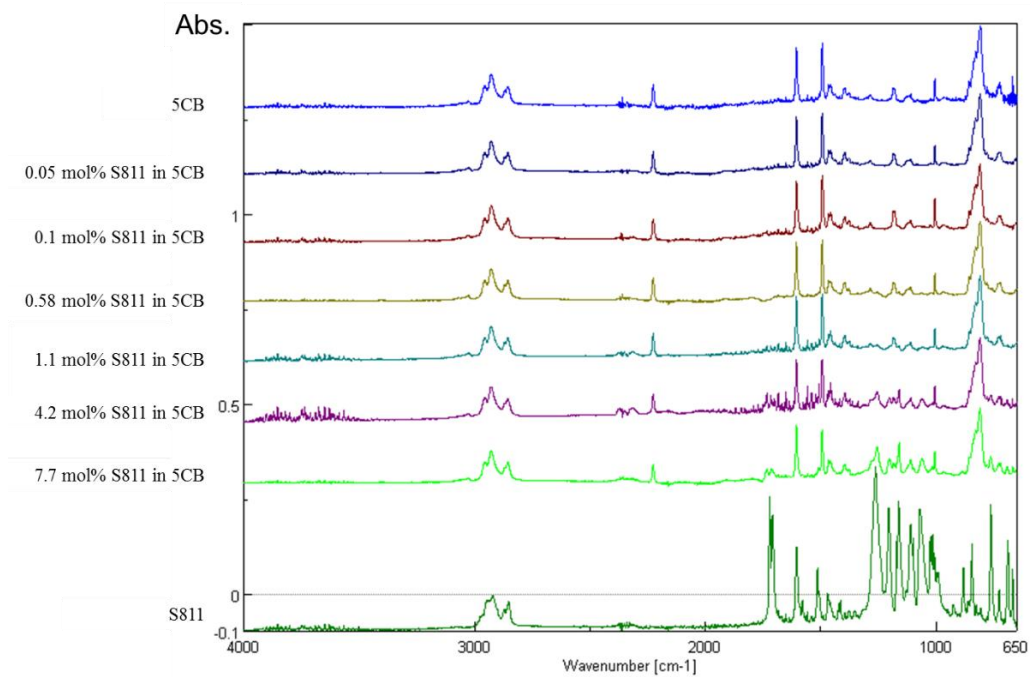


Figure S18 IR spectra of the binary mixtures of 5CB and S811. Measurements were done at RT with an ATR unit.

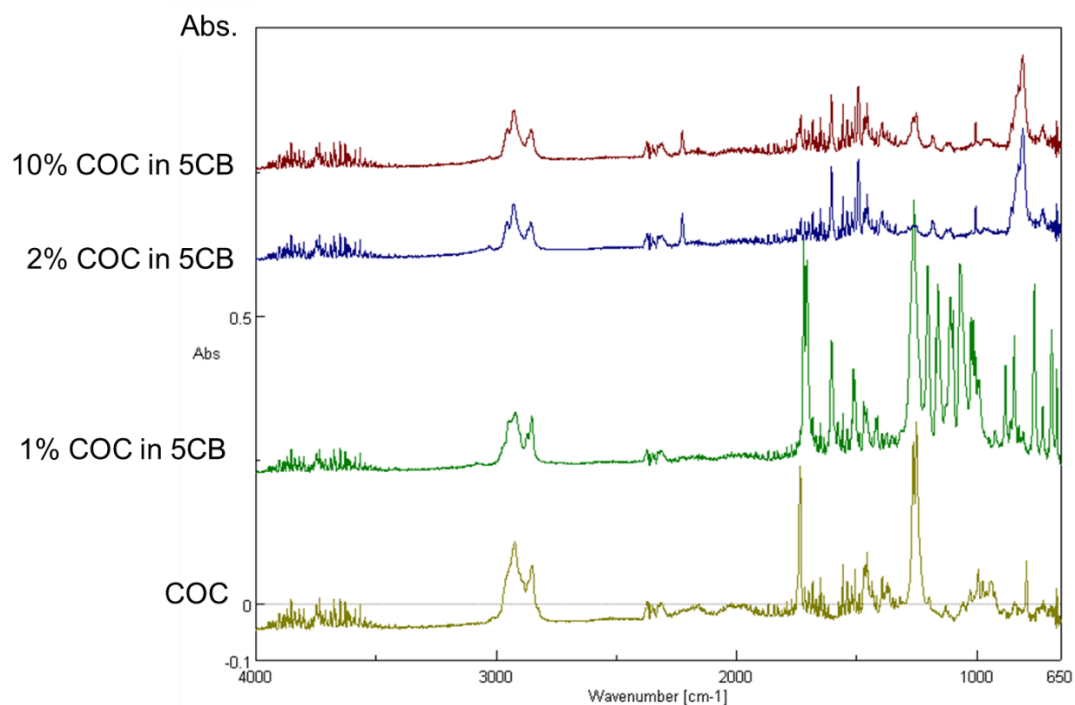


Figure S19 IR spectra of the binary mixtures of 5CB and COC. Measurements were done at RT with an ATR unit.

Raman spectra

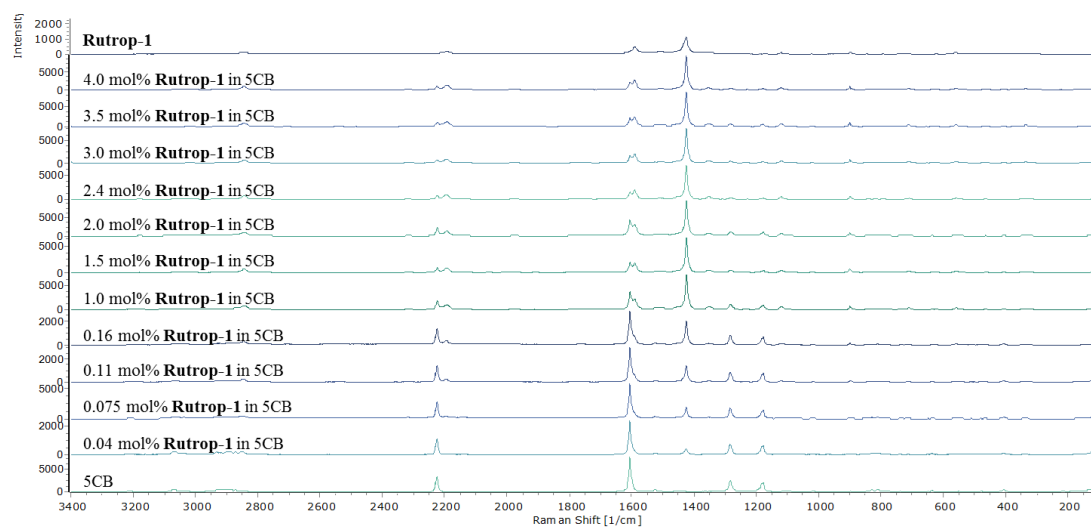


Figure S20 Raman spectra of the binary mixtures of Δ -Rutrop-1 and 5CB. The dopant concentration ranges from 0.04 to 4.0 mol%.

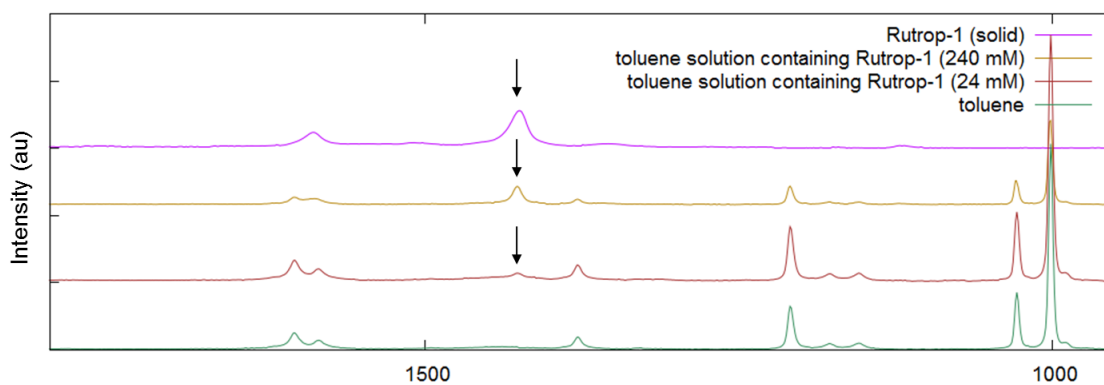


Figure S 21 Raman spectra of toluene solution containing Δ -Rutrop-1 (240 and 24 mM).

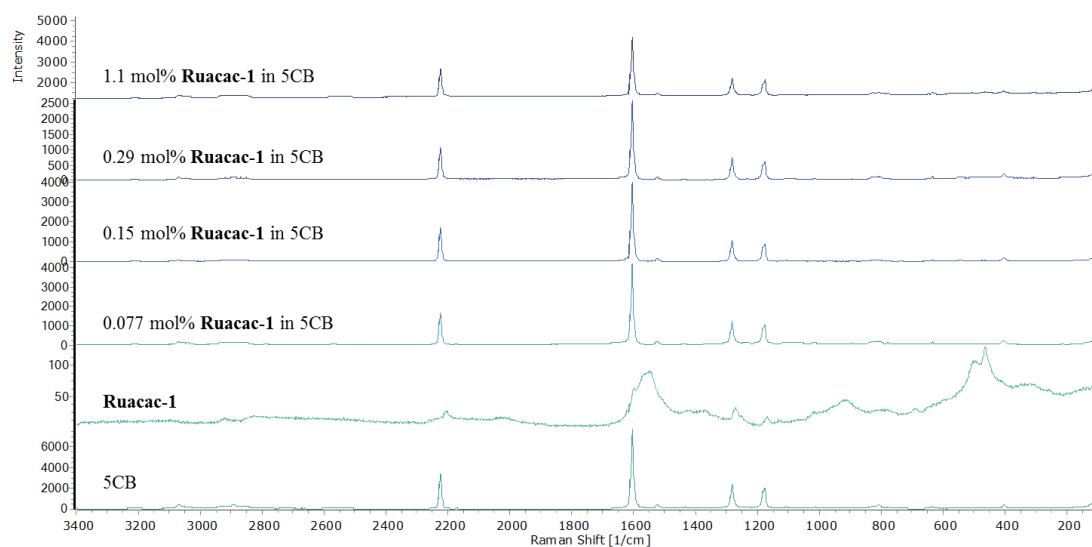


Figure S22 Raman spectra of the binary mixtures of Δ -**Ruacac-1** and 5CB. The dopant concentration ranges from 0.077 to 1.1 mol%.

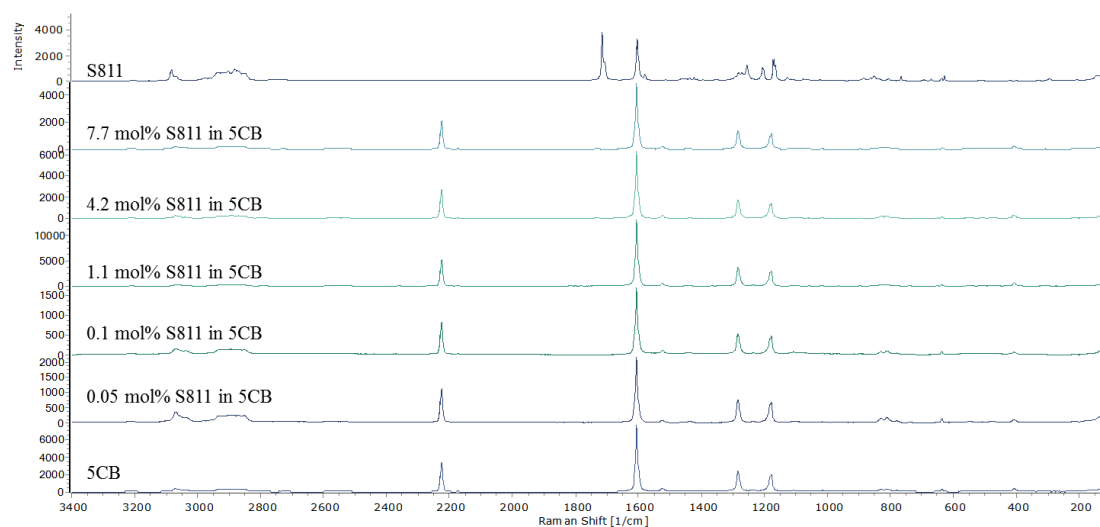


Figure S 23 Raman spectra of the binary mixtures of S-811 and 5CB. The dopant concentration ranges from 0.05 to 7.7 mol%.

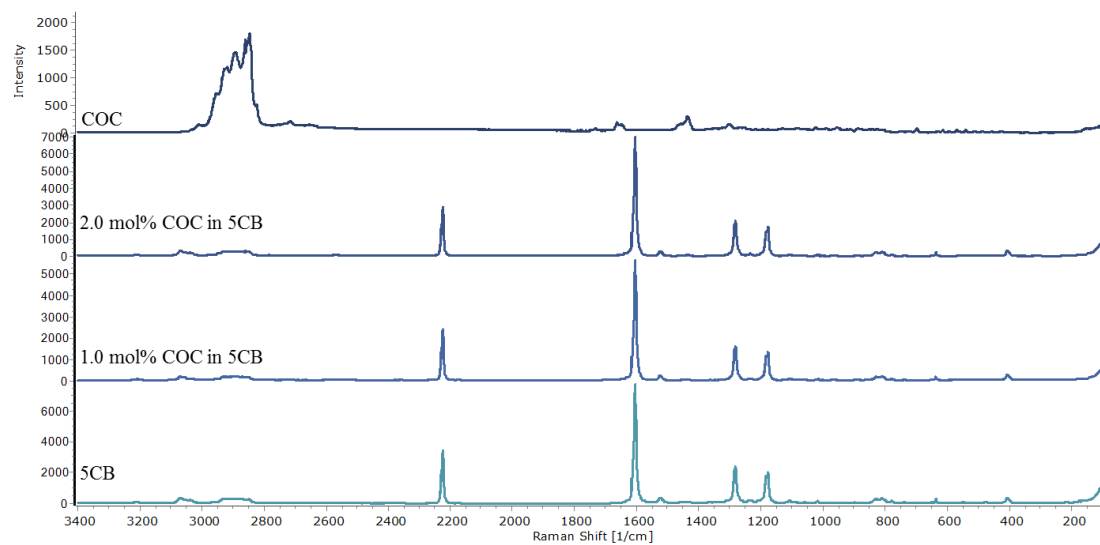


Figure S24 Raman spectra of the binary mixtures of COC and 5CB. The dopant concentrations are 1.0 and 2.0 mol%.

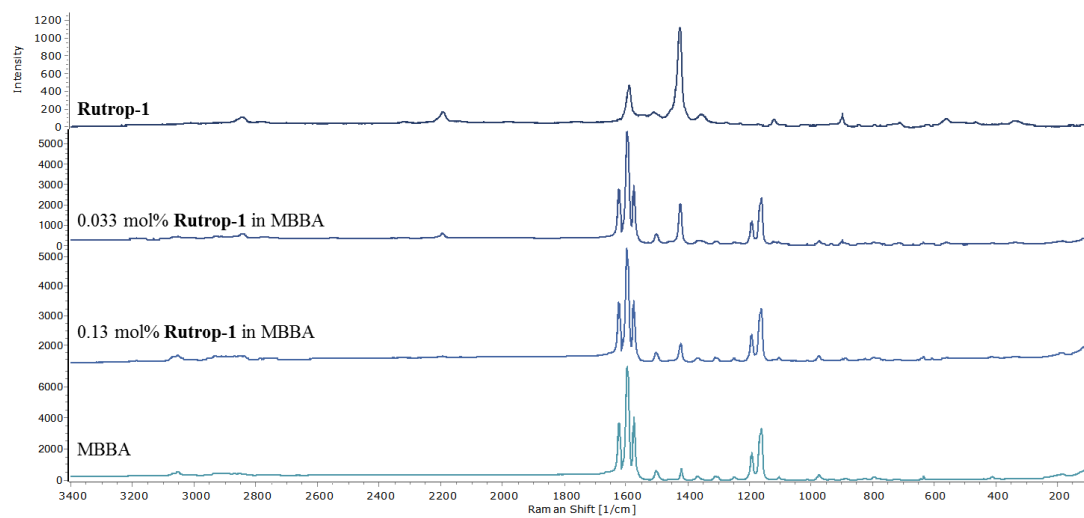


Figure S25 Raman spectra of the binary mixtures of Δ -Rutrop-1 and MBBA (0.033 and 0.13 mol%).

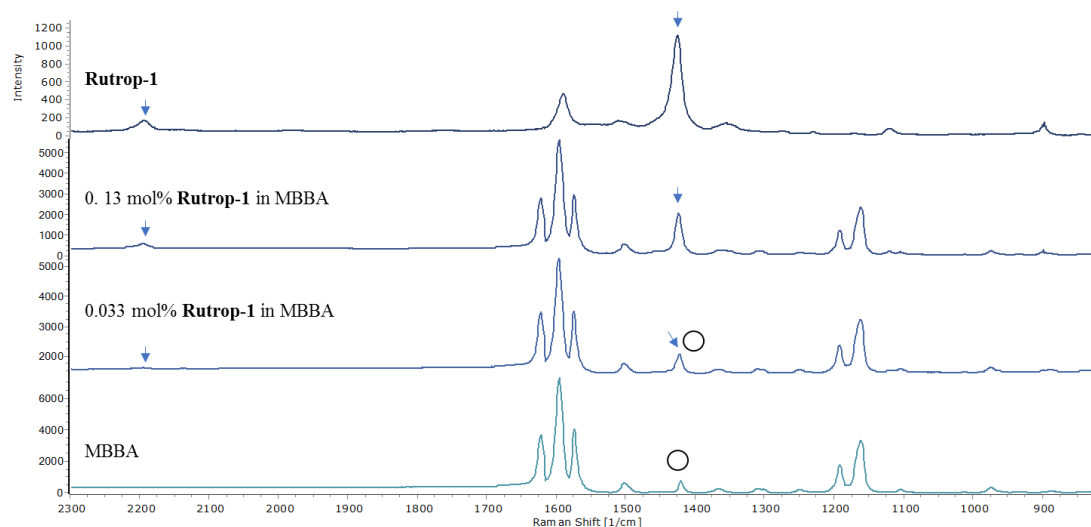


Figure S26 Enlarged view of Raman spectra of the binary mixtures of Δ -**Rutrop-1** and MBBA. The signals marked with arrows and circles correspond to Δ -**Rutrop-1** and MBBA, respectively.

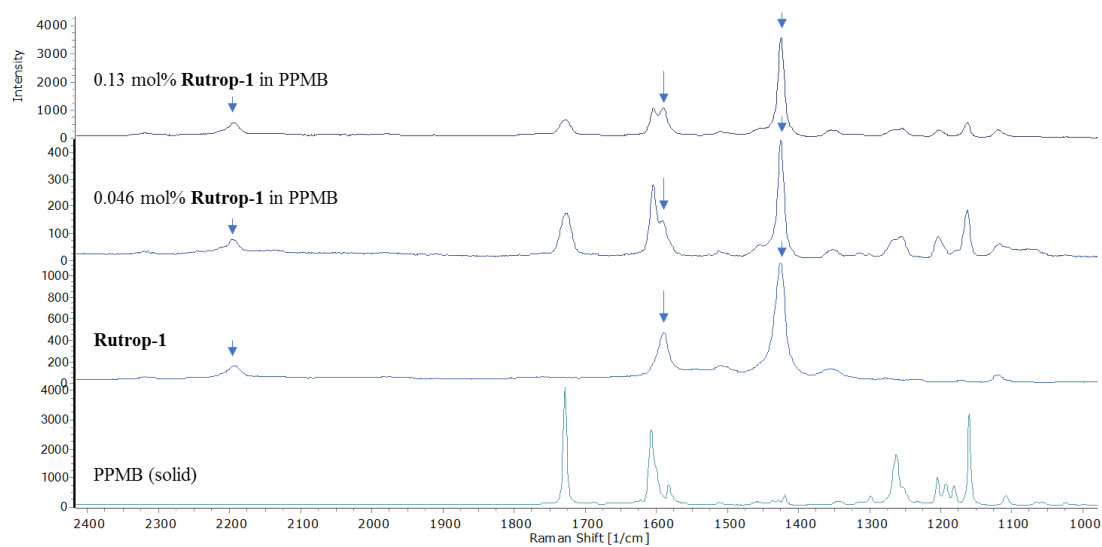


Figure S 27 Raman spectra of the binary mixtures of Δ -**Rutrop-1** and PPMB (0.046 and 0.13 mol%). The signals marked with arrows correspond to Δ -**Rutrop-1**.

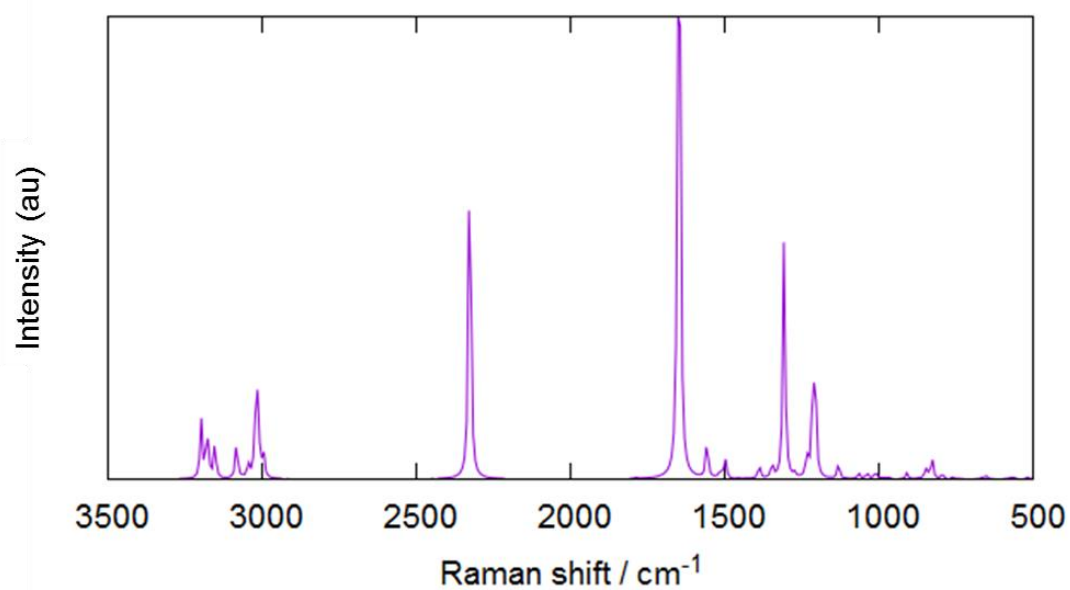


Figure S28 Calculated Raman spectrum of **Rutrop-1** by DFT with UMPW1PW91 functional and 6-311G(d) basis sets for C, H, O and LanL2DZ for Ru (Condition 05 in **Table S1**).

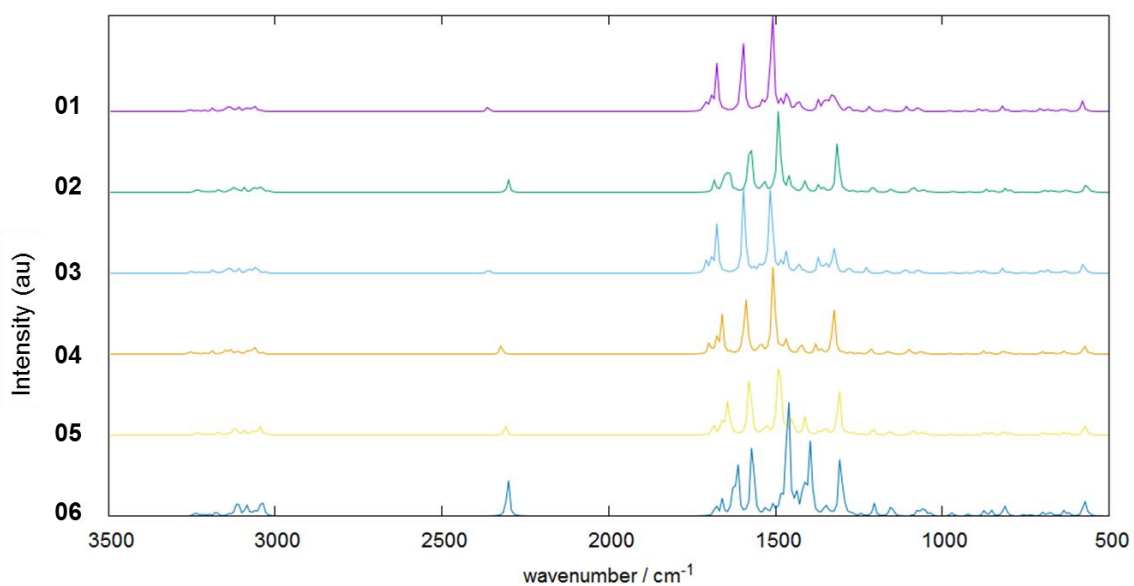


Figure S 29 IR spectra of **Rutrop-1** calculated at different conditions. The numbers of the left side correspond to the calculation conditions (**Table S1**).

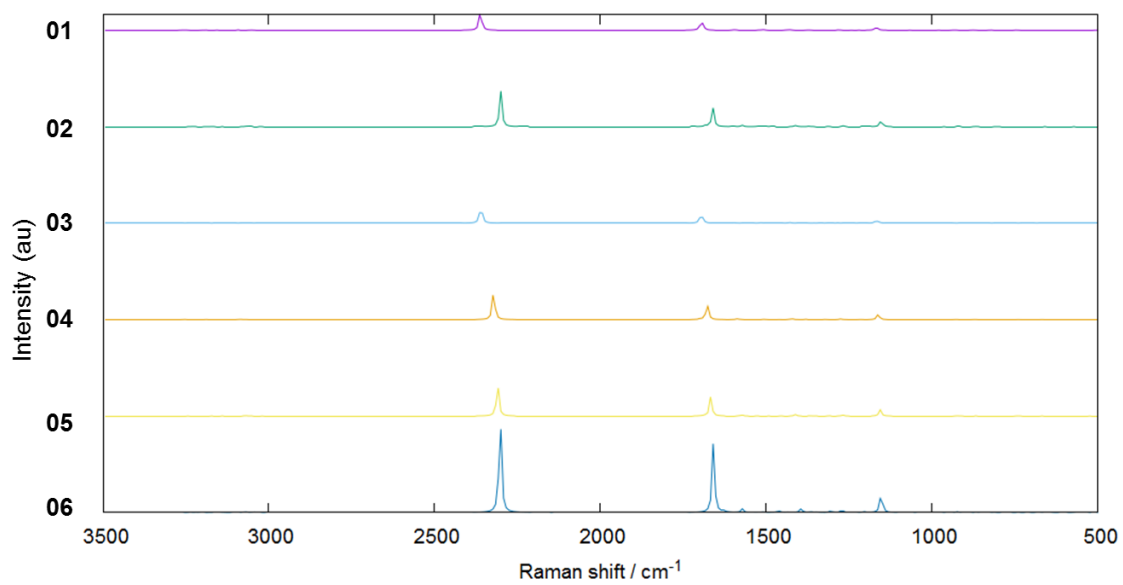


Figure S 30 Raman spectra of **Rutrop-1** calculated at different conditions. The numbers of the left side correspond to the calculation conditions (**Table S1**).

Polarized optical microscope images

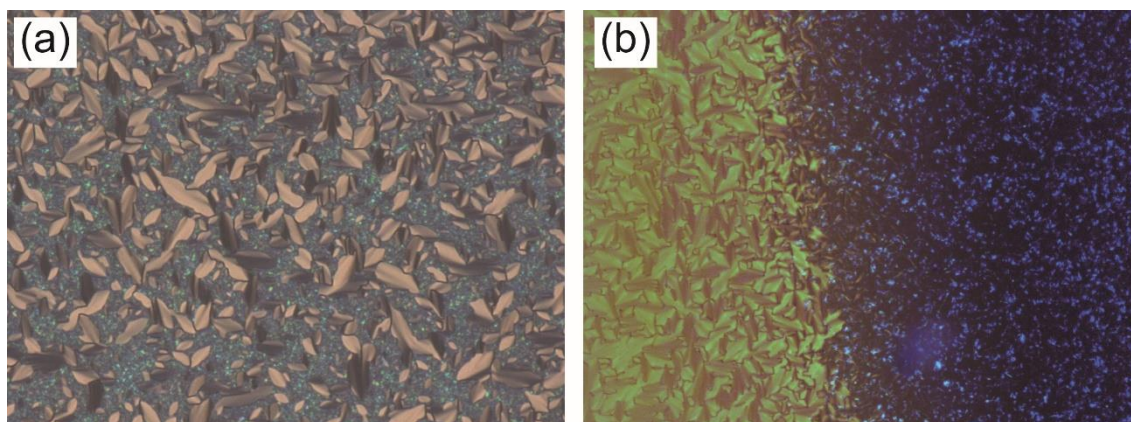


Figure S31 Polarized optical microscope images of (a) 3.6 mol% and (b) 4.0 mol% Δ -Rutrop-1 at the co-existent state of mixture of BP and N* phases (100 \times magnification) taken with reflected light.

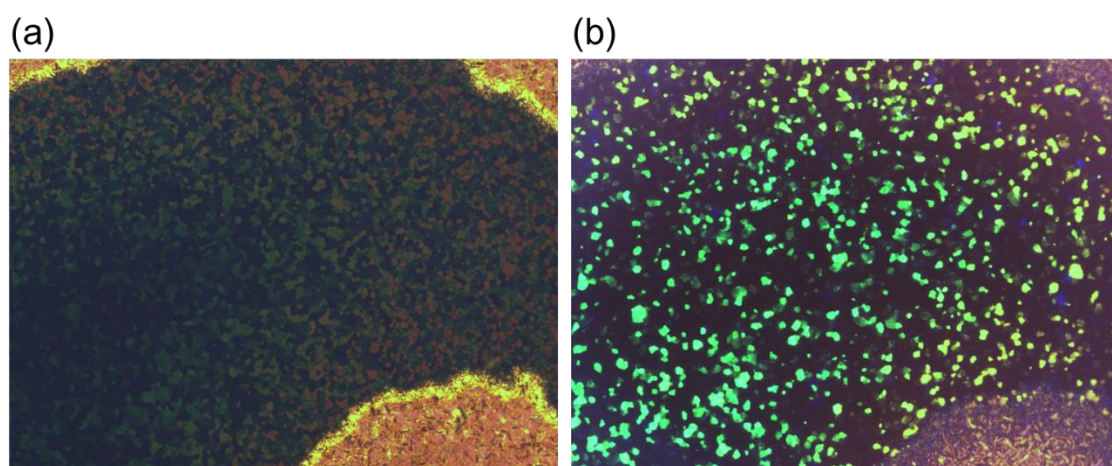


Figure S32 Polarized optical microscope images of a binary mixture of 3.8 mol% Δ -Rutrop-1 and MBBA (100 \times magnification) at BP taken with (a) transmitted and (b) reflected light.



Figure S33 Polarized optical microscope images of a binary mixture of 3.8 mol% Δ -Rutrop-1 and MBBA showing a color perturbation at BP (100 \times magnification) taken with reflected light.

References

- 1 Y. Long, H. Chen, Y. Yang, H. Wang, Y. Yang, N. Li, K. Li, J. Pei and F. Liu, *Macromolecules*, 2009, **42**, 6501–6509.
- 2 J. Yoshida, K. Kuwahara and H. Yuge, *J. Organomet. Chem.*, 2014, **756**, 19–26.
- 3 H. Matsuzawa, Y. Ohashi, Y. Kaizu and H. Kobayashi, *Inorg. Chem.*, 1988, **27**, 2981–2985.
- 4 H. Kobayashi, H. Matsuzawa, Y. Kaizu and A. Ichida, *Inorg. Chem.*, 1987, **26**, 4318–4323.
- 5 I. I. Smalyukh and O. D. Lavrentovich, *Phys. Rev. E*, 2002, **66**, 1–16.
- 6 Frisch, M. J.; Trucks, G. W.; Schlegel, H. B.; Scuseria, G. E.; Robb, M. A.; Cheeseman, J. R.; Scalmani, G.; Barone, V.; Mennucci, B.; Petersson, G. A.; Nakatsuji, H.; Caricato, M.; Li, X.; Hratchian, H. P.; Izmaylov, A. F.; Bloino, J.; Zheng, G.; Sonnenberg, J. L.; Hada, M.; Ehara, M.; Toyota, K.; Fukuda, R.; Hasegawa, J.; Ishida, M.; Nakajima, T.; Honda, Y.; Kitao, O.; Nakai, H.; Vreven, T.; Montgomery, J. A., Jr.; Peralta, J. E.; Ogliaro, F.; Bearpark, M.; Heyd, J. J.; Brothers, E.; Kudin, K. N.; Staroverov, V. N.; Kobayashi, R.; Normand, J.; Raghavachari, K.; Rendell, A.; Burant, J. C.; Iyengar, S. S.; Tomasi, J.; Cossi, M.; Rega, N.; Millam, J. M.; Klene, M.; Knox, J. E.; Cross, J. B.; Bakken, V.; Adamo, C.; Jaramillo, J.; Gomperts, R.; Stratmann, R. E.; Yazyev, O.; Austin, A. J.; Cammi, R.; Pomelli, C.; Ochterski, J. W.; Martin, R. L.; Morokuma, K.; Zakrzewski, V. G.; Voth, G. A.; Salvador, P.; Dannenberg, J. J.; Dapprich, S.; Daniels, A. D.; Farkas, Ö.; Foresman, J. B.; Ortiz, J. V.; Cioslowski, J.; Fox, D. J. Gaussian 09, Revision D.01. *Gaussian Inc., Wallingford*. 2009.
- 7 V. Barone, M. Cossi and J. Tomasi, *J. Chem. Phys.*, 1997, **107**, 3210–3221.
- 8 M. Cossi, G. Scalmani, N. Rega and V. Barone, *J. Chem. Phys.*, 2002, **117**, 43–54.